DOE/NETL Review Meeting April 10, 201

# Ceramic Hollow Fiber Membrane Reactor for Air Separation and Oxygen Production

PI: Xingjian (Chris) Xue
Dept. of Mechanical Engineering and SOFC program
University of South Carolina, Columbia, SC

# Technology and Aims

- Technology aims :
  - enhance production rate of high-purity oxygen from air;
  - Improve stability and reliability;
  - Reduce cost.

Working principle of ceramic membrane for oxygen permeation

**Feed (air) side** $0.5O_2 + 2e^- \rightarrow O^{2-}$

**Membrane** ↓$O^{2-}$ ↓$O^{2-}$ ↓$O^{2-}$ ↓$O^{2-}$ ↑$e^-$ ↑$e^-$ ↑$e^-$ ↑$e^-$

**Permeate (oxygen) side** $O^{2-} \rightarrow 0.5O_2 + 2e^-$

- At the feed (oxygen rich) side :
  - oxygen molecule combines with electrons from the permeate (oxygen lean) side, thereby being reduced to oxygen ion;
  - generated oxygen ion jumps into oxygen vacancy in dense membrane and migrates to the permeate side;
- At the permeate side (oxygen lean):
  - oxygen ion is oxidized to form $O_2$ and release electrons;
  - released electrons at the permeate side then transport back to the feed side, forming a closed-circuit loop within the membrane.

# Technology in a gasification/CTL plant

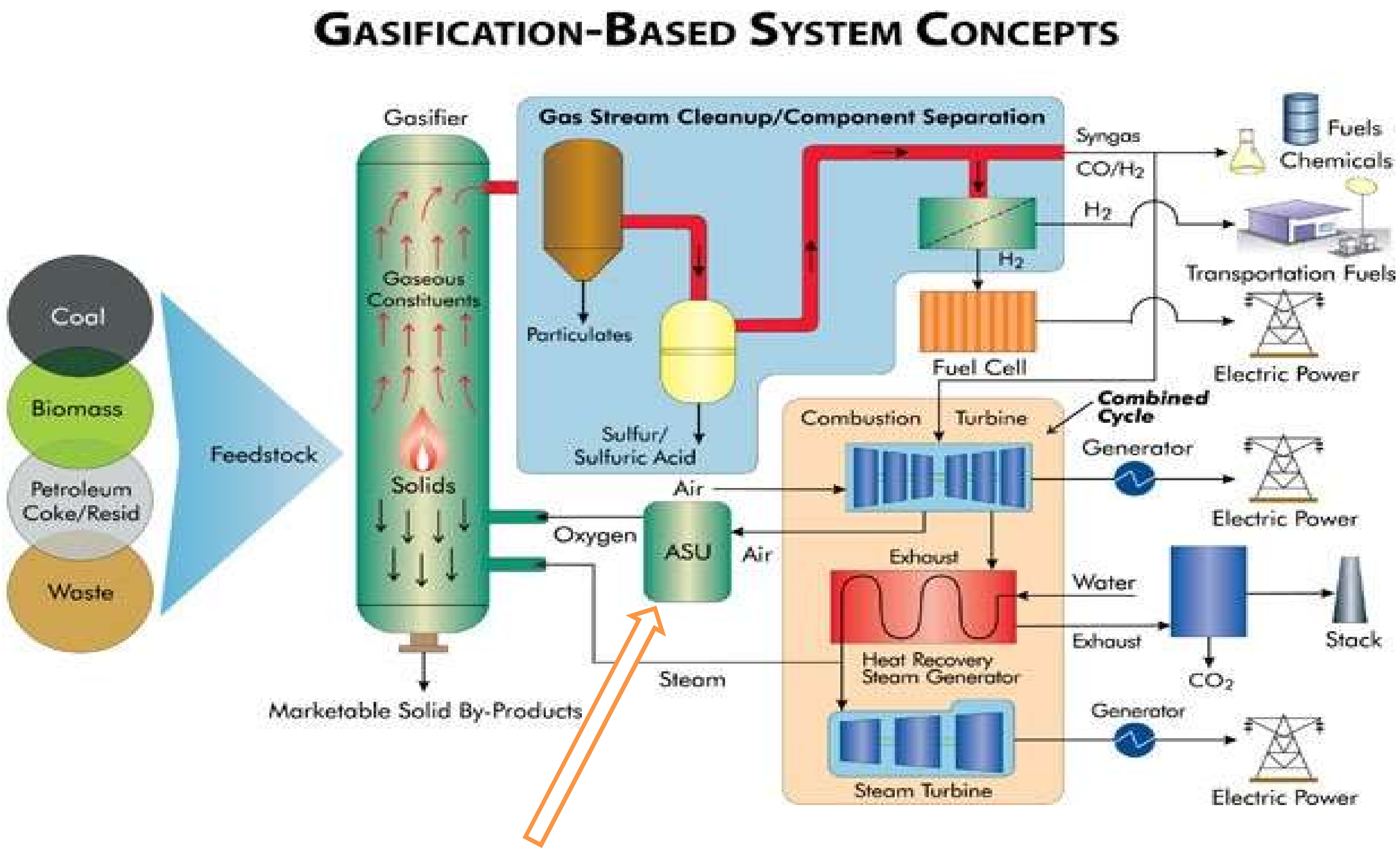


***<u>Membrane module should be located here</u>***

This figure is adopted from the Office of Fossil Energy, Energy.gov

# Project Goals and Commercial Viability

*<u>Project goals:</u>*

- *Mixed conducting materials with high electrochemical kinetic properties;*
- *Novel hollow fiber membrane design and fabrication;*
- *Membrane stack and module development.*

*<u>Advantages and commercial viability:</u>*

- *Improve specific oxygen flux and enhance permeation performance;*
- *Reduce system and operating cost;*
- *Improve robustness and reliability;*
- *Up-scaling flexibility for various applications.*

# Membrane Materials

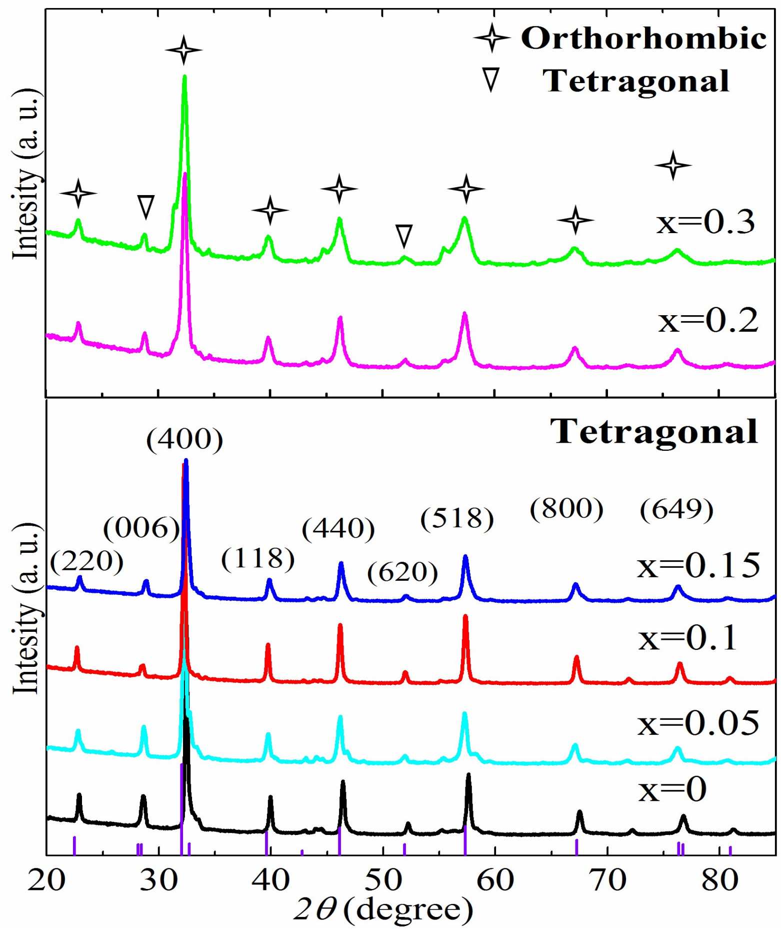


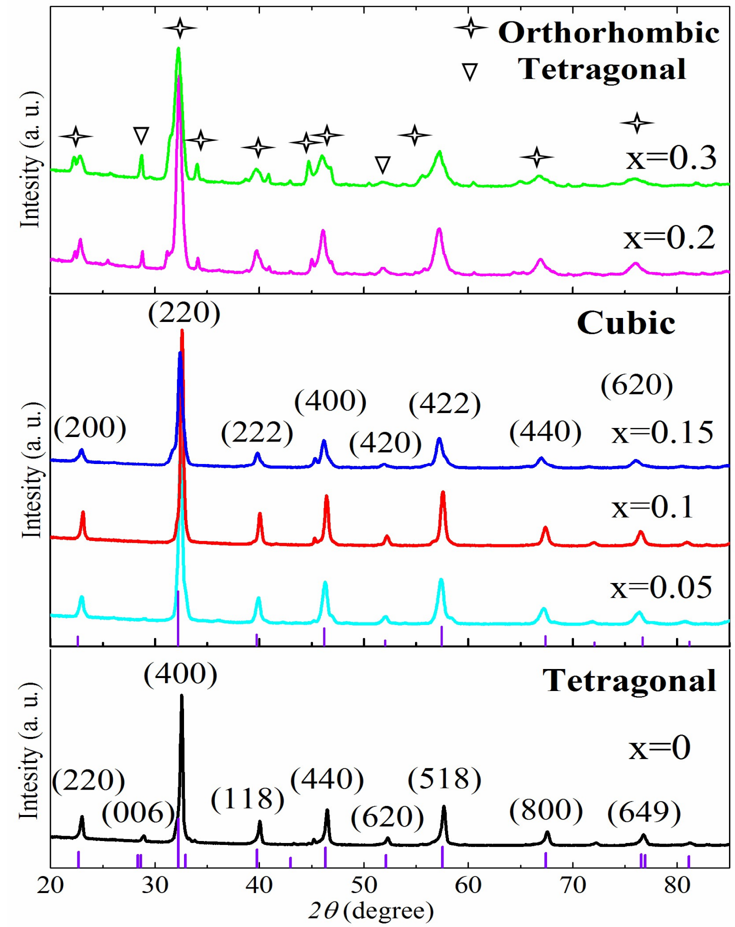


- The XRD patterns of as-prepared $PrBaFe_{(2-x)}Sn_xO_{5+\delta}$ (x=0, 0.05, 0.1, 0.15, 0.2, 0.3) powder samples calcinated at 1000 $^oC$ for 6 h in air.
- The XRD patterns of $PrBaFe_{(2-x)}Sn_xO_{5+\delta}$ after reducing treatment at 800 $^oC$ for 24h in humidified gas mixture $H_2/N_2$ with $H_2:N_2$ = 1:9 (volume ratio).

# Membrane Materials

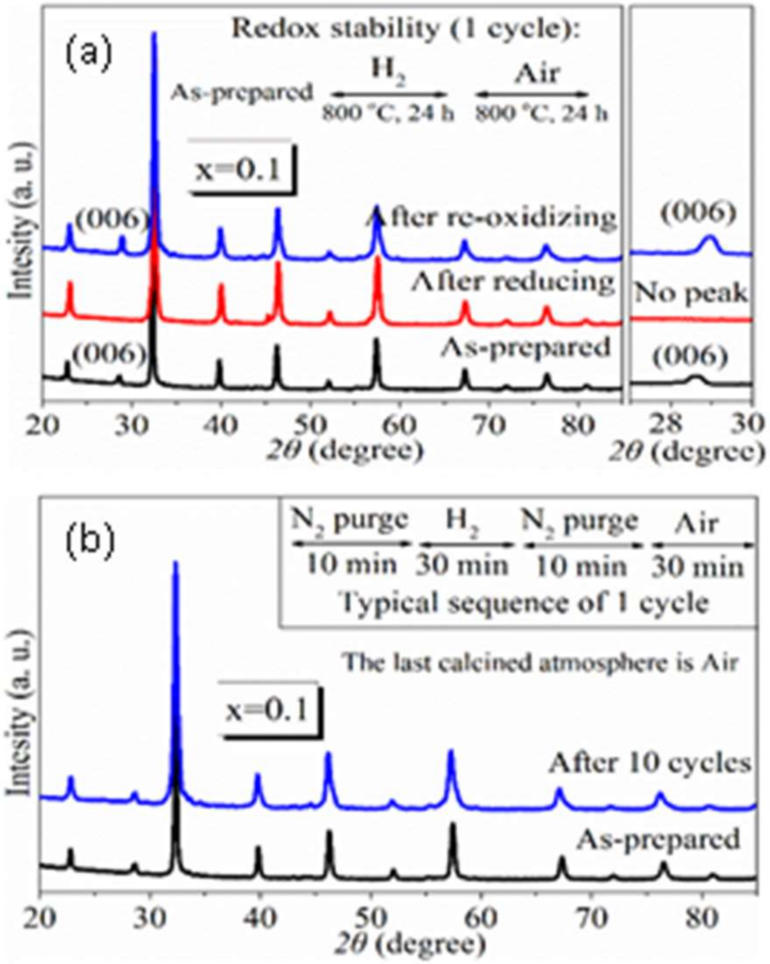


- The XRD patterns of $PrBaFe_{(2-x)}Sn_xO_{5+\delta}$ (x=0.1) at different stages of redox cycles at 800 °C.

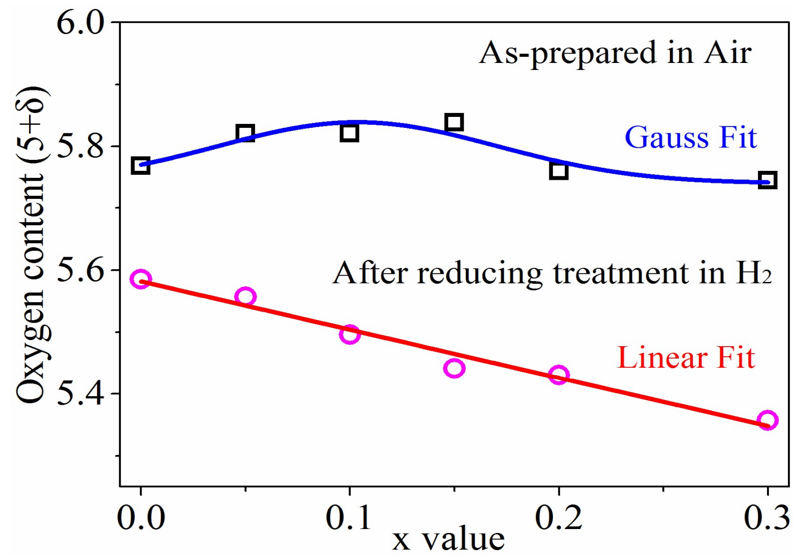


- The oxygen content (5+δ) as a function of x value in $PrBaFe_{(2-x)}Sn_xO_{5+\delta}$ (x=0, 0.05, 0.1, 0.15, 0.2, 0.3) before and after reducing treatment at 800 °C for 24h in humidified gas mixture of 10%$H_2$ + 90%$N_2$.

# Membrane Materials

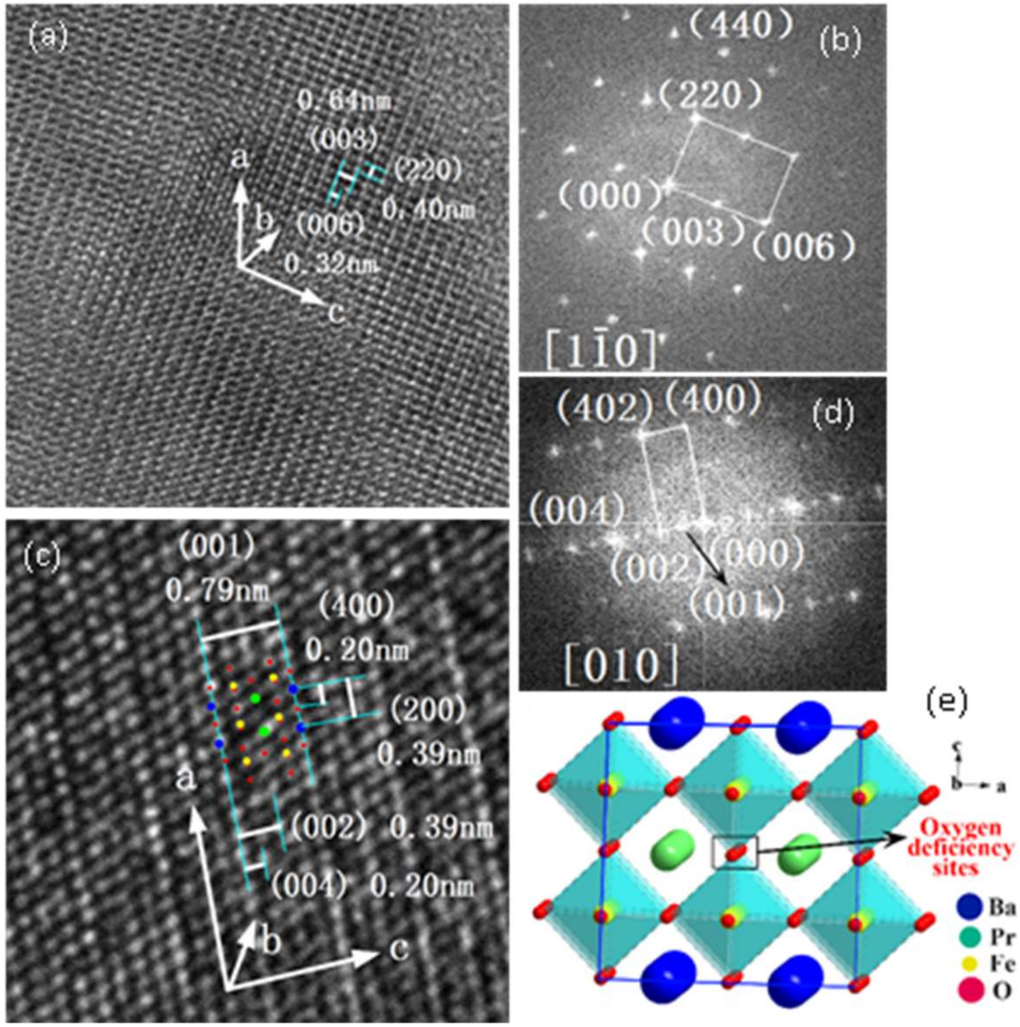


- HR-TEM images, FFT and schematic illustration of crystal structure of $PrBaFe_{(2-x)}Sn_xO_{5+\delta}$ (x=0.1). (a,b) HR-TEM image and FFT before reducing treatment; (c,d) HR-TEM image and FFT after reducing treatment; (e) schematic representation of double perovskite $PrBaFe_2O_{5+\delta}$.

# Membrane Materials

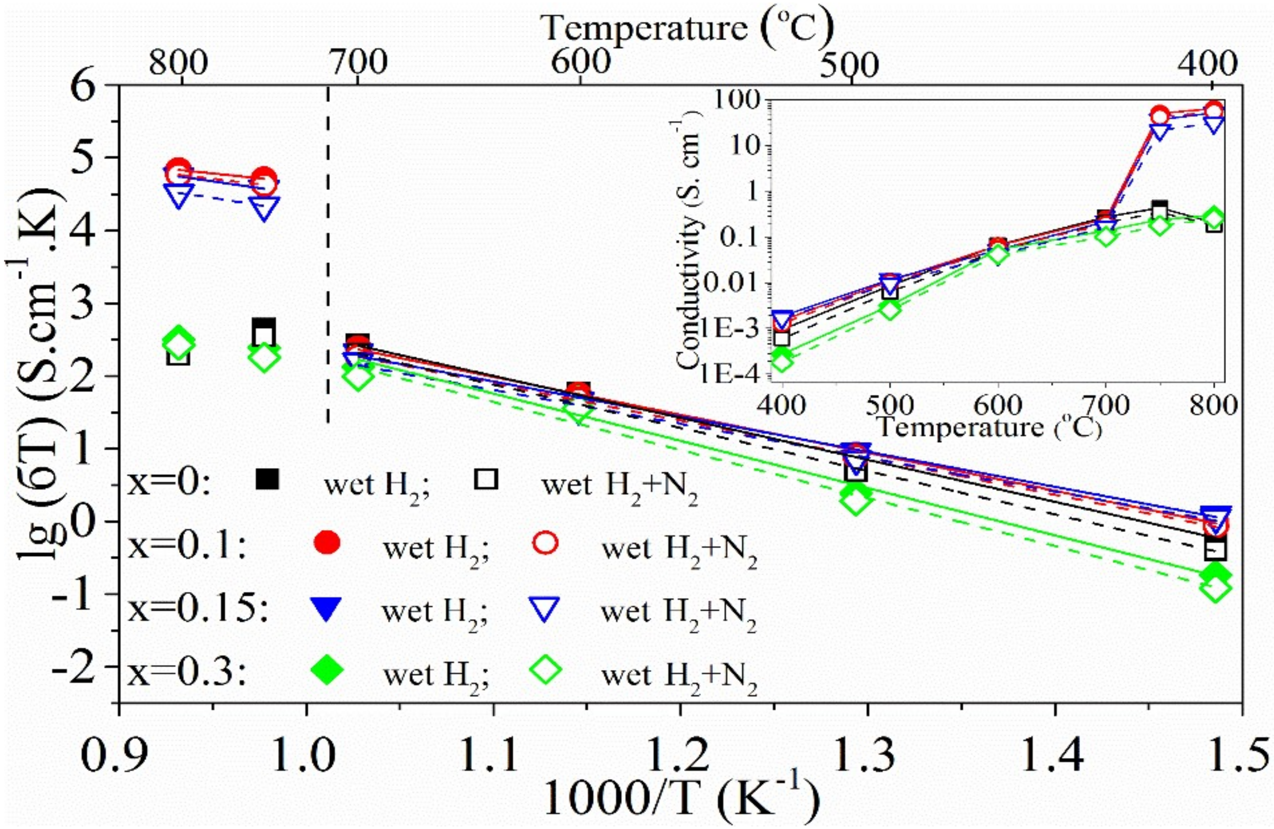


| Atomsphere | Sn doping amount | | | | | | | |
|---|---|---|---|---|---|---|---|---|
| | x=0 | | x=0.1 | | x=0.15 | | x=0.3 | |
| | $H_2$ | $H_2+N_2$ | $H_2$ | $H_2+N_2$ | $H_2$ | $H_2+N_2$ | $H_2$ | $H_2+N_2$ |
| Ea (eV): 400-700 °C | 1.14 | 1.18 | 1.03 | 1.01 | 0.96 | 0.92 | 1.29 | 1.31 |
| Ea (eV): 750-800 °C | / | / | 0.53 | 0.59 | 0.74 | 0.77 | / | / |

# Membrane Materials

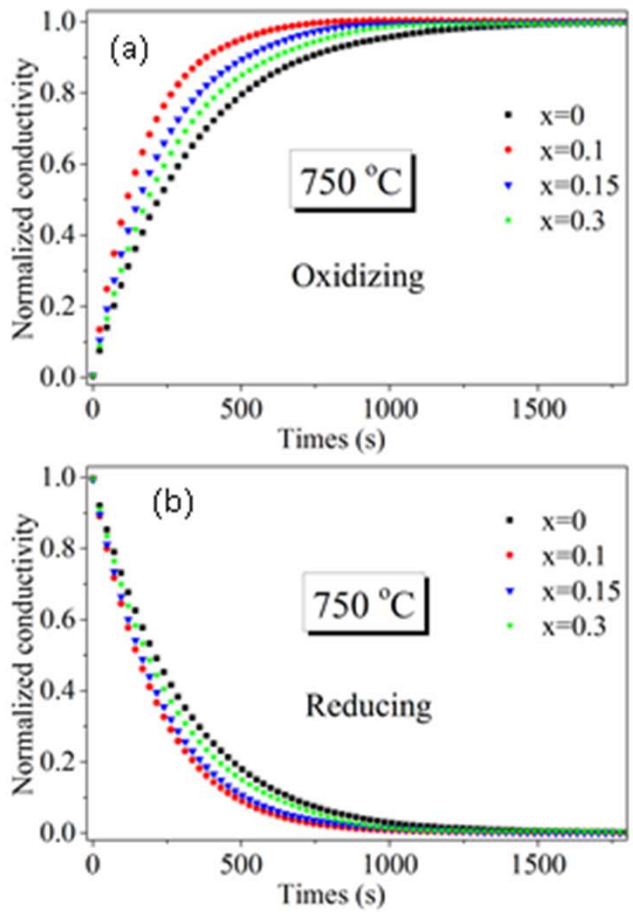


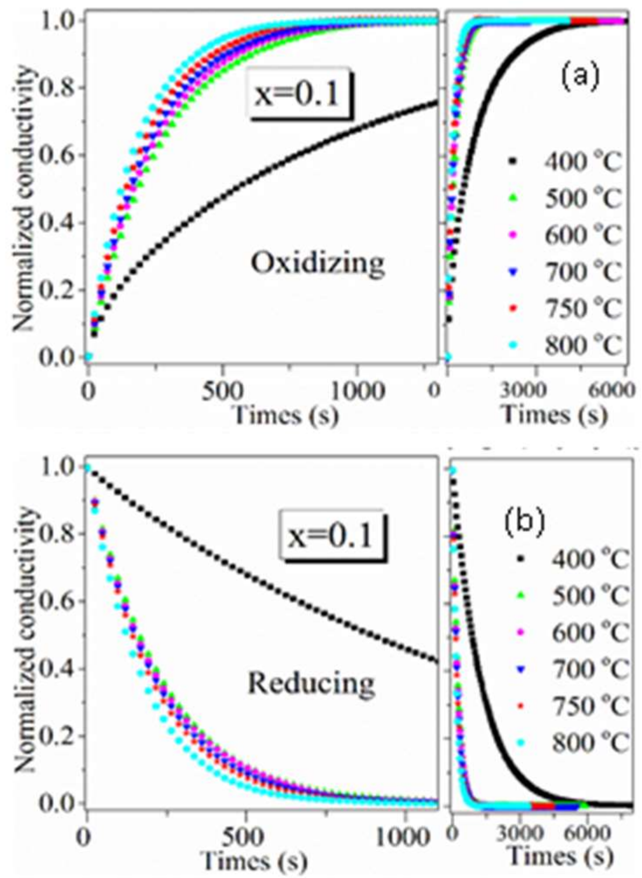


- Normalized ECR behaviors of bulk $PrBaFe_{(2-x)}Sn_xO_{5+\delta}$ (x=0, 0.1, 0.15, 0.3) at 750 °C between humidified $H_2$ and humidified $50\%H_2+50\%N_2$.

- Normalized ECR behaviors of bulk $PrBaFe_{(2-x)}Sn_xO_{5+\delta}$ (x = 0.1) at 400 –800 °C between humidified $H_2$ and humidified $50\%H_2+50\%N_2$.

# Membrane Materials

| Step change of oxygen partial pressure | Sn doping amount | | | | | | | |
|---|---|---|---|---|---|---|---|---|
| | x=0 | | x=0.1 | | x=0.15 | | x=0.3 | |
| | $k_{ex}$ ($10^{-6}$ m $s^{-1}$) | $D_{chem}$ ($10^{-7}$ $m^2s^{-1}$) | $k_{ex}$ ($10^{-6}$ m $s^{-1}$) | $D_{chem}$ ($10^{-7}$ $m^2s^{-1}$) | $k_{ex}$ ($10^{-6}$ m $s^{-1}$) | $D_{chem}$ ($10^{-7}$ $m^2s^{-1}$) | $k_{ex}$ ($10^{-6}$ m $s^{-1}$) | $D_{chem}$ ($10^{-7}$ $m^2s^{-1}$) |
| $H_2 \rightarrow H_2+N_2$ | 2.30 | 0.57 | 3.56 | 4.22 | 3.28 | 3.12 | 2.76 | 1.58 |
| $H_2+N_2 \rightarrow H_2$ | 2.98 | 3.14 | 4.42 | 6.04 | 3.32 | 5.52 | 3.18 | 4.27 |

Surface exchange coefficient ($k_{ex}$) and bulk diffusivity ($D_{chem}$) of $PrBaFe_{(2-x)}Sn_xO_{5+\delta}$ (x=0, 0.1, 0.15, 0.3) extracted from ECR experimental data at 750 °C.

| Step change of oxygen partial pressure | Operating Temperature | | | | | | | | | | | |
|---|---|---|---|---|---|---|---|---|---|---|---|---|
| | 400 °C | | 500 °C | | 600 °C | | 700 °C | | 750 °C | | 800 °C | |
| | $k_{ex}$ ($10^{-6}$ m $s^{-1}$) | $D_{chem}$ ($10^{-10}$ $m^2s^{-1}$) | $k_{ex}$ ($10^{-6}$ m $s^{-1}$) | $D_{chem}$ ($10^{-7}$ $m^2s^{-1}$) | $k_{ex}$ ($10^{-6}$ m $s^{-1}$) | $D_{chem}$ ($10^{-7}$ $m^2s^{-1}$) | $k_{ex}$ ($10^{-6}$ m $s^{-1}$) | $D_{chem}$ ($10^{-7}$ $m^2s^{-1}$) | $k_{ex}$ ($10^{-6}$ m $s^{-1}$) | $D_{chem}$ ($10^{-7}$ $m^2s^{-1}$) | $k_{ex}$ ($10^{-6}$ m $s^{-1}$) | $D_{chem}$ ($10^{-7}$ $m^2s^{-1}$) |
| $H_2 \rightarrow H_2+N_2$ | 0.59 | 3.72 | 1.31 | 1.5 | 2.31 | 2.74 | 3.02 | 3.48 | 3.56 | 4.22 | 4.35 | 5.34 |
| $H_2+N_2 \rightarrow H_2$ | 1.08 | 2.92 | 2.65 | 3.58 | 3.16 | 3.85 | 4.05 | 5.39 | 4.42 | 6.04 | 4.97 | 6.70 |

Surface exchange coefficient ($k_{ex}$) and bulk diffusivity ($D_{chem}$) of $PrBaFe_{(2-x)}Sn_xO_{5+\delta}$ (x=0.1) extracted from ECR experimental data at 400 – 800 °C.

# Membrane Materials

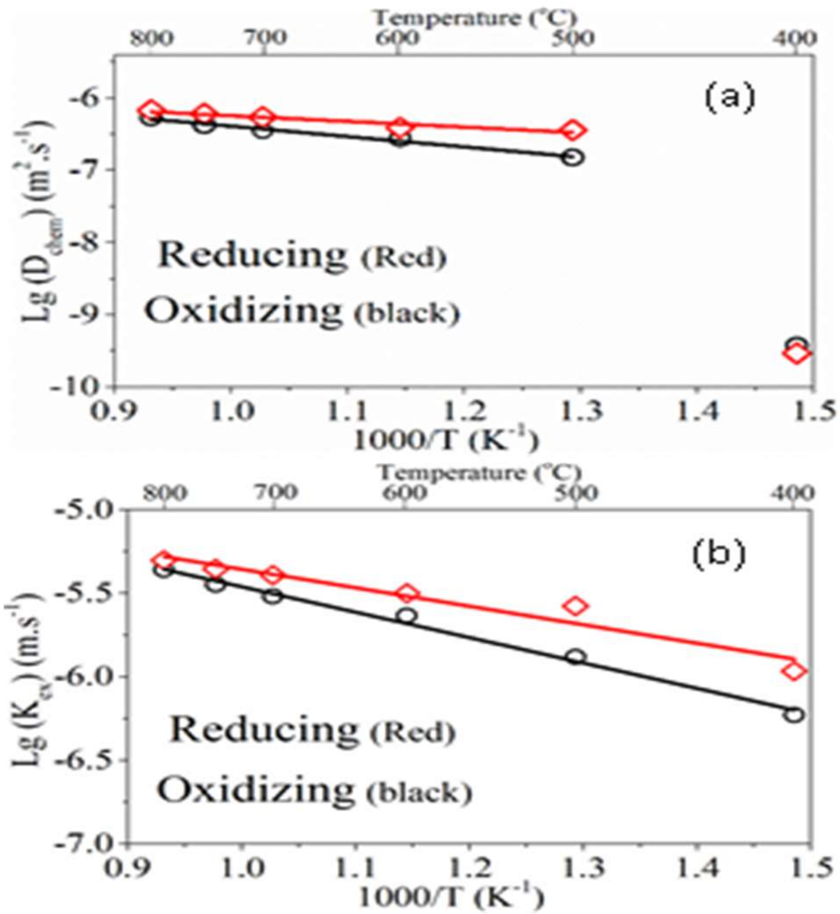


- Arrhenius plots of (a) bulk diffusivity $D_{chem}$ and (b) surface exchange coefficient $K_{ex}$ of $PrBaFe_{(2-x)}Sn_xO_{5+\delta}$ (x=0.1) when the surrounding atmosphere changes from humidified $H_2$ to humidified mixture of 50%$H_2$+50%$N_2$ (black), and from humidified mixture of 50%$H_2$+50%$N_2$ to humidified $H_2$ (red).

# Membrane Materials

| Electrode | Electrolyte | Temperature (°C) | ASR ($\Omega$ cm$^2$) |
|---|---|---|---|
| Ni-YSZ | YSZ | 800 | 0.16 |
| $La_{0.75}Sr_{0.25}Cr_{0.5}Mn_{0.5}O_3$ | YSZ | 900 | 0.26 |
| $Sr_2Fe_{1.5}Mo_{0.5}O_{6-\delta}$ | LSGM | 850 | 0.21 |
| $Sr_2MgMoO_{6-\delta}$ | LSGM | 850 | 0.48 |
| $Sr_2Co_{1.1}Mo_{0.9}O_{6-\delta}$ | LSGM | 800 | ~0.35 |
| $La_4Sr_8Ti_{11}Mn_{0.5}Ga_{0.5}O_{38-\delta}$/YSZ | YSZ | 850 | ~0.25 |
| $Sr_2FeMo_{0.65}Ni_{0.35}O_{6-\delta}$ | LSGM | 850 | 0.106 |
| | | 800 | 0.163 |
| | | 750 | 0.290 |
| $PrBaFe_{1.9}Sn_{0.1}O_{5+\delta}$ | LSGM | 850 | 0.095 |
| | | 800 | 0.141 |
| | | 750 | 0.285 |

- Comparisons of ASRs of the typical anode materials in literature with those of the $PrBaFe_{1.9}Sn_{0.1}O_{5+\delta}$ prepared in this work.

# Fabrication of Hollow Fiber Membranes

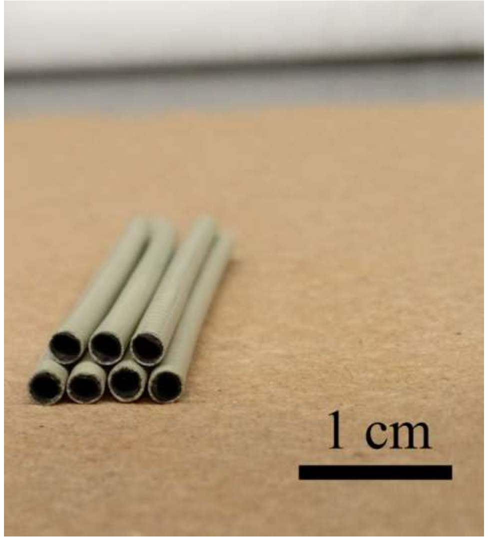

# Fabrication of Hollow Fiber Membranes

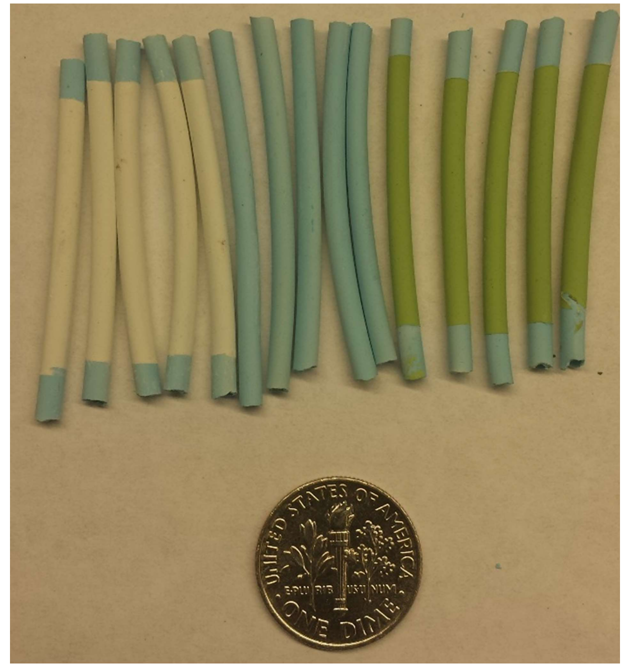

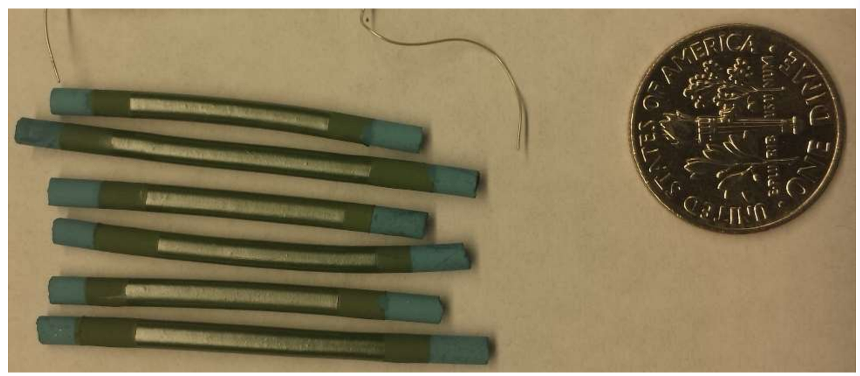

# Fabrication of Hollow Fiber Membranes

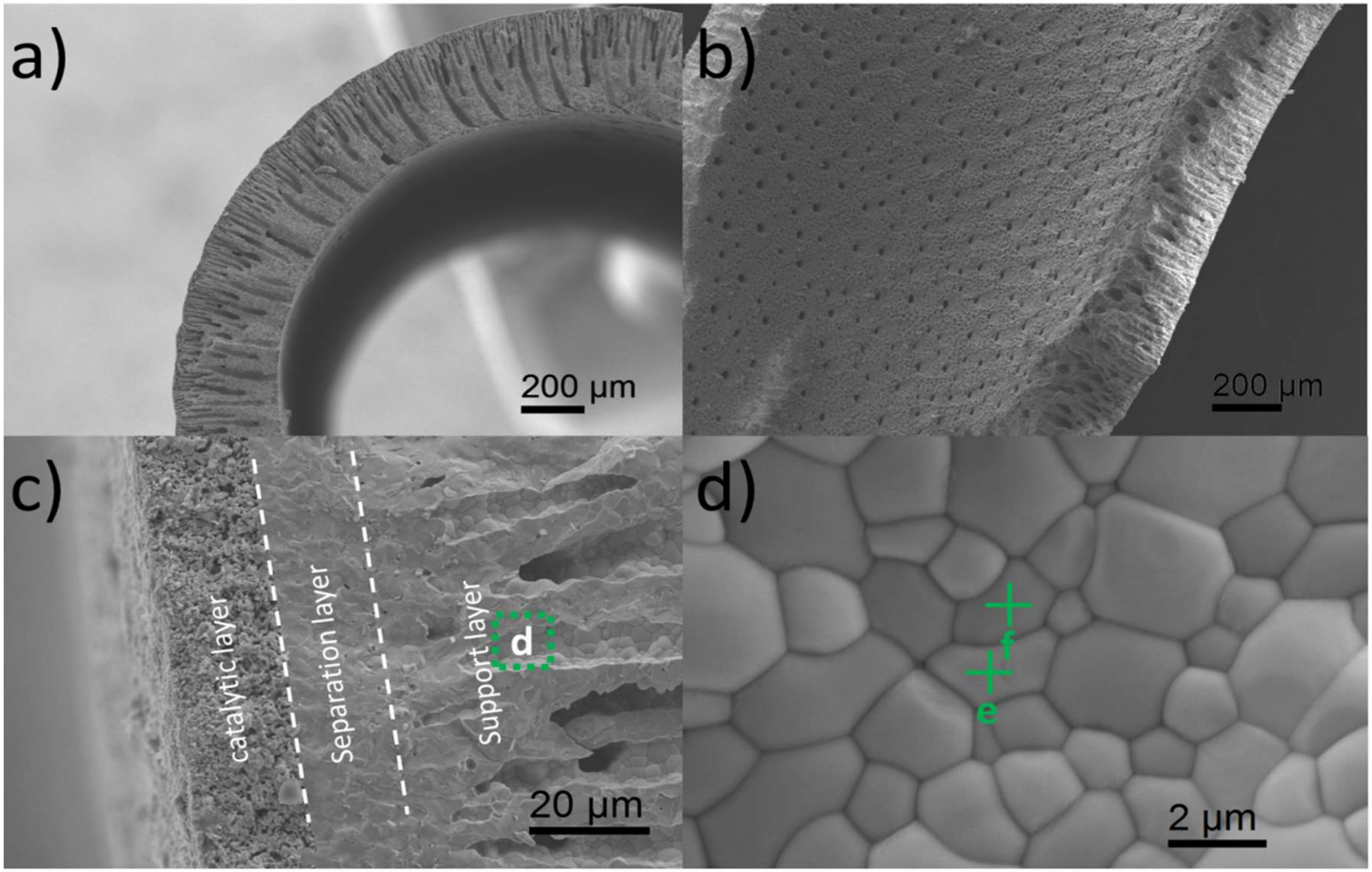

# Performance of Hollow Fiber Membranes

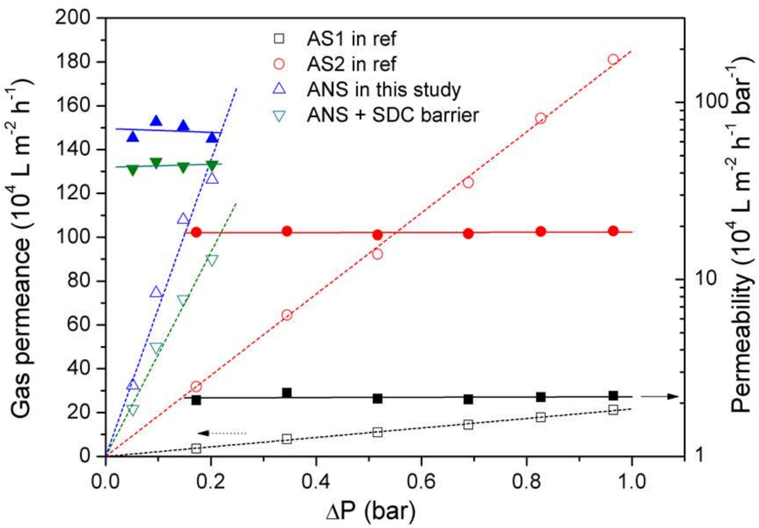


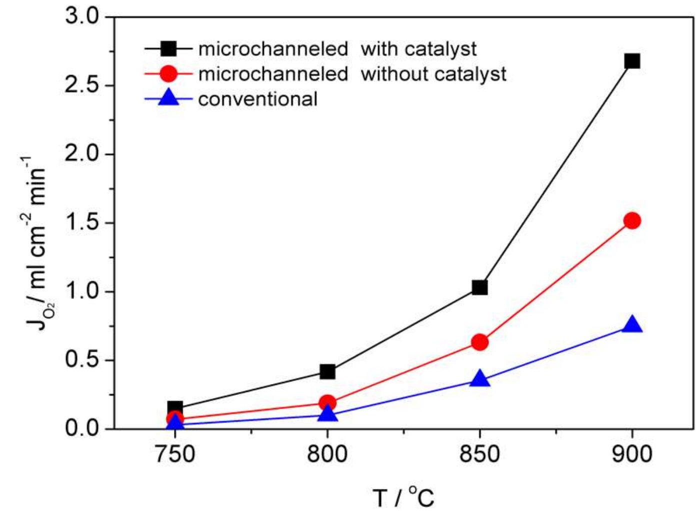


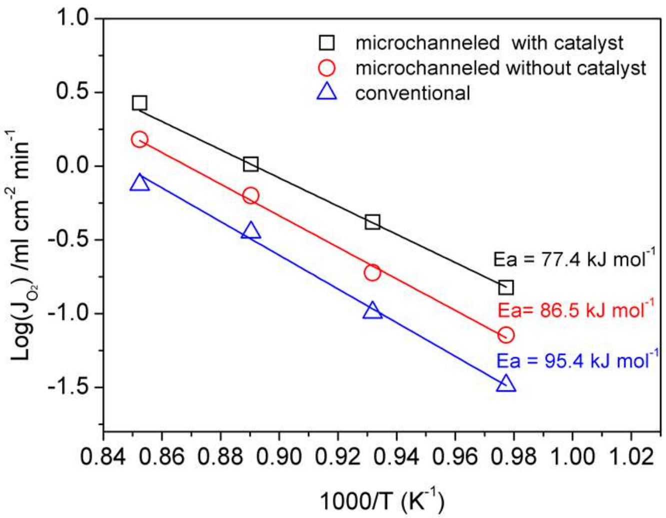


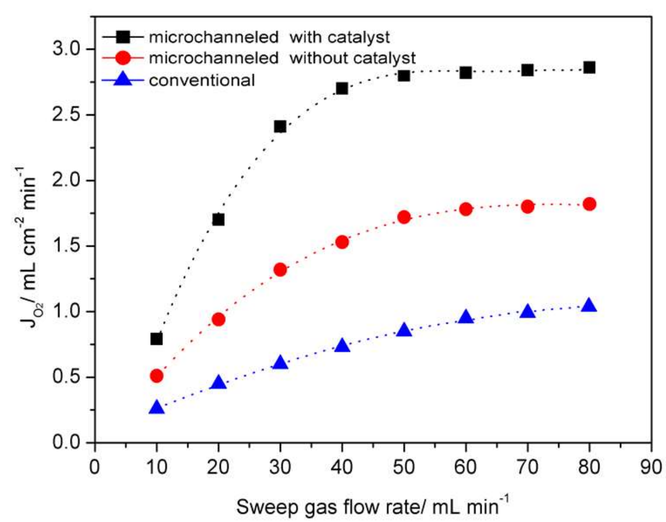

# Performance of Hollow Fiber Membranes

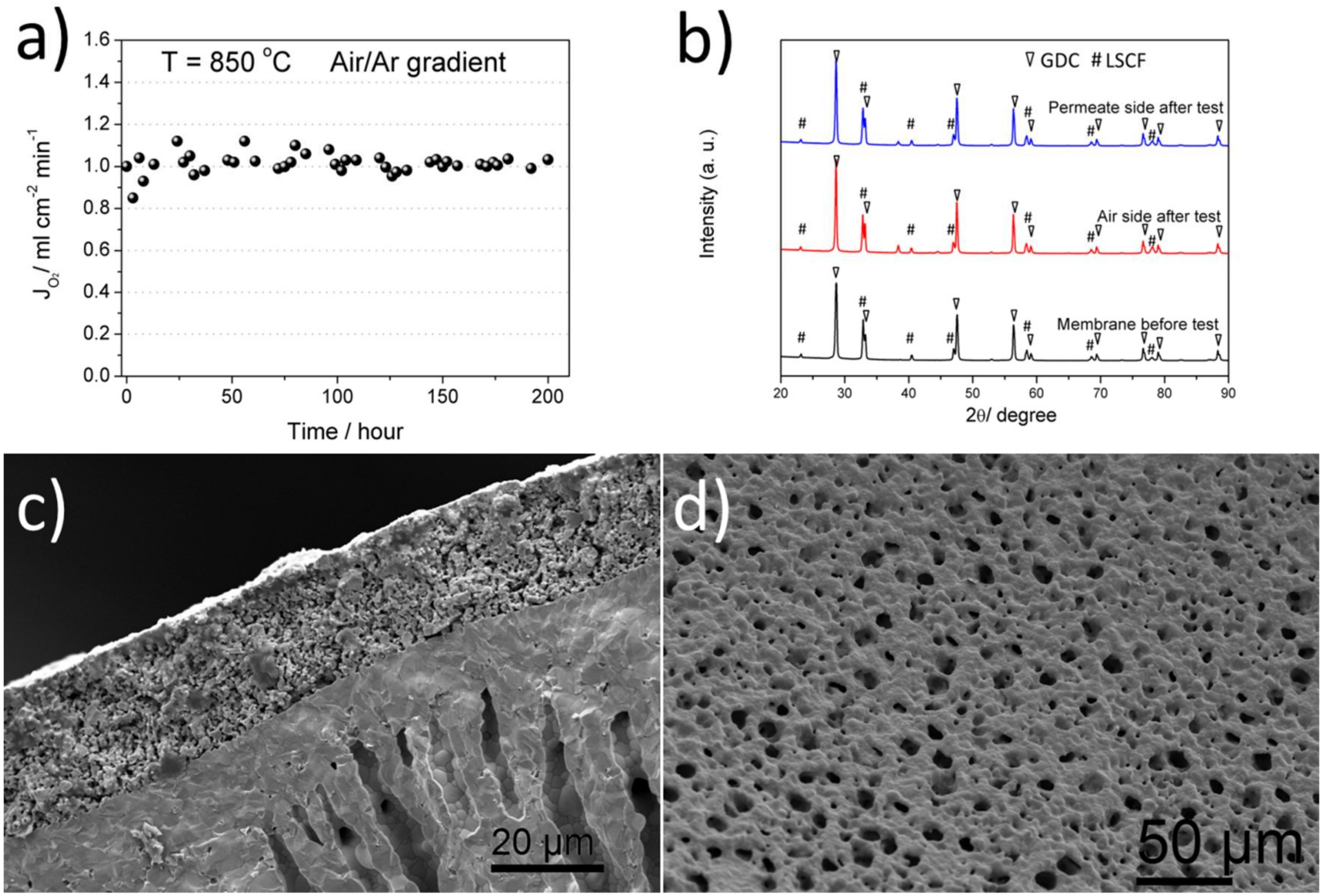

# On-going and future work

- Novel single membranes with new material systems
  - Fabrications;
  - Permeation performance measurement and characterizations;
  - Stability test;
- Stack and module development:
  - Stack design and fabrication;
  - Performance testing
  - Characterizations;
  - Analysis and optimization

# Acknowledgments

DOE/NETL Contract number:
DE-FE0024059, DE-FE0031473

Post-docs and Graduates:
Chunlei Ren
Run Gan
Myongjin Lee
Chunyang Yang
Guohui Dong
Fei He
Yangmei Jiang